

TIME-REVERSAL INVARIANT TOPOLOGICAL INSULATORS

A DISSERTATION  
SUBMITTED TO THE DEPARTMENT OF PHYSICS  
AND THE COMMITTEE ON GRADUATE STUDIES  
OF STANFORD UNIVERSITY  
IN PARTIAL FULFILLMENT OF THE REQUIREMENTS  
FOR THE DEGREE OF  
DOCTOR OF PHILOSOPHY

Taylor L. Hughes

August 2009

## Chapter 2

# Topological Insulators: A Primer

This chapter will serve as an informal tutorial on our research on the general response theory of topological insulators. The material here is based on a set of informal lectures I gave at the Perimeter Institute in May 2009. The arguments here may not be as precise as those in later chapters, but in exchange I will present material that guided our research as well as a broader picture of the general structure of topological insulators in a more conversational tone without focussing on subtle details. The outline of this chapter is as follows: I will first discuss the physics of  $(2 + 1)$ -d time-reversal breaking (TRB) topological insulators and the subsequent dimensional reduction to the  $(1 + 1)$ -d topological insulators. Then I will draw an analogy between this family of insulators and their higher dimensional TRI relatives. Finally, I will give some intuition about the general structure of all of the topological insulator families in any spacetime dimension. The majority of the detailed arguments that I will present can be found in Chapter 6.

## 2.1 Dirac Fermions in $(2 + 1)$ -d and the Half Hall Conductance

We begin by discussing Dirac fermions in  $(2 + 1)$ -d. In this dimension a Dirac fermion has 2 components with a Hamiltonian

$$H_D = p_x \sigma^x + p_y \sigma^y + m \sigma^z \quad (2.1)$$

which can be derived from a field theory Lagrangian density

$$L = \bar{\psi} (i \gamma^\mu \partial_\mu - m) \psi \quad (2.2)$$

$$\bar{\psi} = \psi^\dagger \sigma^z \quad (2.3)$$

$$\gamma^0 = \sigma^z, \quad \gamma^1 = i \sigma^y, \quad \gamma^2 = -i \sigma^x. \quad (2.4)$$

In matrix form we have

$$H_D = \begin{pmatrix} m & p_- \\ p_+ & -m \end{pmatrix}$$

$$p_\pm = p_x \pm i p_y.$$

The energy spectrum is

$$E_\pm = \pm \sqrt{p_x^2 + p_y^2 + m^2} \quad (2.5)$$

with eigenstates

$$\psi = e^{i p \cdot x} \begin{pmatrix} u(p) \\ v(p) \end{pmatrix} \quad (2.6)$$

with a momentum dependent spinor  $(u(p) \ v(p))^T$ .

The parity operation in 2d is

$$P: (x, y) \rightarrow (x, -y). \quad (2.7)$$

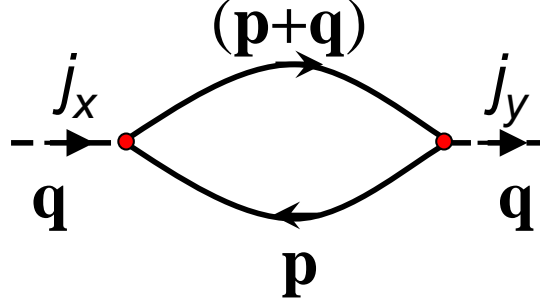


Figure 2.1: Diagram for a current-current correlation function. The vertex operators  $j_i$  are carrying a finite momentum  $\mathbf{q}$ .

The parity operation only flips one coordinate so that the determinant of the transformation will be  $-1$ . If we flipped both coordinates the determinant would be  $+1$  and therefore a rotation. This is a common subtlety seen in even *spatial* dimensions. We want the Hamiltonian to be parity invariant *i.e.*  $PH_D P^{-1} = H_D$  and so we want to pick  $P = \sigma^x$ . Under parity we have

$$\begin{aligned} PH_D(p_x, p_y, m)P^{-1} &= \sigma^x H_D(p_x, -p_y, m)\sigma^x = p_x \sigma^x \sigma^x \sigma^x - p_y \sigma^x \sigma^y \sigma^x + m \sigma^x \sigma^z \sigma^x \\ &= p_x \sigma^x + p_y \sigma^y - m \sigma^z \end{aligned}$$

which implies that the mass term breaks parity explicitly. We can ask the question: is there a physical consequence of the parity breaking?

To examine this we need to couple the system to an electromagnetic field via

$$H_D \rightarrow (p_x + eA_x)\sigma^x + (p_y + eA_y)\sigma^y + m\sigma^z.$$

Since the fermions are massive we can integrate them out to get the effective action

$$\begin{aligned} Z[A] &= \int D\bar{\psi} D\psi e^{iS[\psi, \bar{\psi}, A]} \\ S_{eff}[A] &= -i \log Z[A]. \end{aligned} \tag{2.8}$$

The effective action will let us calculate the response properties of the system to see if the parity breaking influences the electromagnetic behavior. To calculate the physical linear response of the fermions to  $A_\mu$  we calculate the current-current correlation function (see Fig. 2.1). We can calculate the polarization tensor to lowest order by calculating this diagram. We are interested only in the parity violating pieces and so I will only keep terms which are odd in powers of  $m$ . We have

$$\begin{aligned}
\Pi_{\mu\nu} &= \frac{1}{2} \int \frac{d^3p}{(2\pi)^3} \text{Tr} [G(p+q)j_\mu(p+q)G(p)j_\nu(p,p+q)] \\
&= \frac{1}{2} \int \frac{d^3p}{(2\pi)^3} \text{Tr} \left[ \frac{i}{(p_\sigma + q_\sigma)\gamma^\sigma - m} (i\gamma_\mu) \frac{i}{p_\alpha\gamma^\alpha - m} i\gamma_\nu \right] \\
&= \frac{1}{2} \int \frac{d^3p}{(2\pi)^3} \text{Tr} \left[ \frac{(p_\sigma + q_\sigma)\gamma^\sigma + m}{(p+q)^2 - m^2} \gamma_\mu \frac{p_\alpha\gamma^\alpha + m}{p^2 - m^2} \gamma_\nu \right] \\
&= \frac{1}{2} \int \frac{d^3p}{(2\pi)^3} \frac{1}{(p+q)^2 - m^2} \frac{1}{p^2 - m^2} \text{Tr} [m(p_\sigma + q_\sigma)\gamma^\sigma\gamma_\mu\gamma_\nu + mp_\sigma\gamma_\mu\gamma^\sigma\gamma_\nu \\
&\quad + \text{parity invariant terms}] \\
&= \frac{1}{2} \int \frac{d^3p}{(2\pi)^3} \frac{-2im\epsilon^{\mu\nu\sigma}}{[(p+q)^2 - m^2][p^2 - m^2]} [(p^\sigma + q^\sigma) - p^\sigma]. \tag{2.9}
\end{aligned}$$

Now we take the long-wavelength limit, *i.e.*  $q \rightarrow 0$ , to get

$$\begin{aligned}
\Pi_{\mu\nu} &= -imq^\sigma \int \frac{d^3p}{(2\pi)^3} \frac{\epsilon_{\mu\nu\sigma}}{[p^2 - m^2]^2} \\
&= -imq^\sigma \int \frac{d\omega d^2p}{(2\pi)^3} \frac{\epsilon_{\mu\nu\sigma}}{[\omega^2 - p_x^2 - p_y^2 - m^2]^2} \\
&= -mq^\sigma \int \frac{d\omega_E d^2p}{(2\pi)^3} \frac{\epsilon_{\mu\nu\sigma}}{[\omega_E^2 + p_x^2 + p_y^2 + m^2]^2} \\
&= -\frac{m\pi}{2(2\pi)^3} q^\sigma \epsilon_{\mu\nu\sigma} \int \frac{|p|d\theta d|p|}{(|p|^2 + m^2)^2} \\
&= -\frac{m}{8\pi} q^\sigma \epsilon_{\mu\nu\sigma} \int \frac{|p|d|p|}{(|p|^2 + m^2)^2} \\
&= -\frac{m}{8\pi|m|} q^\sigma \epsilon_{\mu\nu\sigma} = -\frac{\text{sgn}(m)}{8\pi} q^\sigma \epsilon_{\mu\nu\sigma}. \tag{2.10}
\end{aligned}$$

Having this term in the polarization kernel implies that there is a term in the effective

action of the form

$$S_{eff}[A] = -\frac{1}{8\pi} \text{sgn}(m) \int d^3x \epsilon^{\mu\sigma\nu} A_\mu \partial_\sigma A_\nu + \text{parity invariant terms} \quad (2.11)$$

To find the current we simply need to take a functional derivative of the effective action

$$j^\mu = \frac{\delta S_{eff}[A]}{\delta A_\mu} = \frac{1}{4\pi} \text{sgn}(m) \epsilon^{\mu\sigma\nu} \partial_\sigma A_\nu \quad (2.12)$$

$$\begin{aligned} \implies j^x &= \frac{1}{4\pi} \text{sgn}(m) (\partial_0 A_y - \partial_y A_0) \\ &= -\frac{1}{4\pi} \text{sgn}(m) E^y. \end{aligned} \quad (2.13)$$

This means that the system has a non-zero Hall conductance

$$\begin{aligned} \sigma_{xy} &= -\frac{\text{sgn}(m)}{4\pi} = -\frac{\text{sgn}(m)e^2}{4\pi\hbar} \\ &= -\frac{1}{2} \frac{e^2}{h} \text{sgn}(m) \end{aligned} \quad (2.14)$$

where we have restored the physical units. We see that the Hall conductance of the (2 + 1)-d Dirac fermions is equal to *half* of the conductance quantum. Not only this, but even in the parity invariant limit  $m \rightarrow 0$  the current does not vanish. This implies that the parity symmetry is broken on the quantum level *i.e.* there is a *parity* anomaly.

A non-zero quantized Hall conductance is usually a result of a non-trivial topological structure in the energy spectrum. Here, with  $p_x, p_y$  as good quantum numbers we can look at the energy spectrum as a function of momenta. The easiest way to see the non-trivial topological configuration is to rewrite the Hamiltonian as

$$H_D = d_a(p) \sigma^a \quad (2.15)$$

$$d_a(p) = (p_x, p_y, m). \quad (2.16)$$

Then we can plot the unit vector field

$$\hat{d}_a(p) = \frac{1}{\sqrt{p_x^2 + p_y^2 + m^2}} (p_x, p_y, m) \quad (2.17)$$

in the  $(p_x, p_y)$  plane. Near the origin, for  $m > 0$  the vector points upward. At infinity the vector field points in the plane and points in the  $\hat{p}$  direction winding around the circle at infinity. This configuration is a *meron*, similar to what is seen in Fig. 3.2. It has half the topological charge of a *skyrmion* and this is connected to the *half* quantized Hall conductance which effectively counts the amount of skyrmion charge.

Before we move on to the lattice Dirac model it is useful to note the Hall conductance of multiple Dirac fermions. If we have  $N$  flavors of Dirac fermions then we get

$$\sigma_{xy} = - \sum_{i=1}^N \frac{e^2}{2h} \text{sgn}(m_i). \quad (2.18)$$

### 2.1.1 Lattice Dirac Model in $(2 + 1)$ -d

We will now consider a square lattice with two fermion degrees of freedom on each lattice site. The lattice Dirac Hamiltonian is

$$\begin{aligned} H_{LD} = & \sum_{m,n} \left\{ \left[ i c_{m+1,n}^\dagger \sigma^x c_{m,n} - i c_{m,n}^\dagger \sigma^x c_{m+1,n} \right] + \left[ i c_{m,n+1}^\dagger \sigma^y c_{m,n} - i c_{m,n}^\dagger \sigma^y c_{m,n+1} \right] \right. \\ & - \left[ c_{m+1,n}^\dagger \sigma^z c_{m,n} + c_{m,n}^\dagger \sigma^z c_{m+1,n} + c_{m,n+1}^\dagger \sigma^z c_{m,n} + c_{m,n}^\dagger \sigma^z c_{m,n+1} \right] \\ & \left. + (2 - m) c_{m,n}^\dagger \sigma^z c_{m,n} \right\} \end{aligned} \quad (2.19)$$

where  $c_{m,n} = (c_{u,m,n} \ c_{v,m,n})$  for the two degrees of freedom  $u, v$ . Now if we assume we have periodic boundary conditions along  $x$  and  $y$  we can Fourier transform the fermion operators using

$$c_{m,n} = \frac{1}{\sqrt{L_x L_y}} \sum_{p_x, p_y} e^{i(p_x m + p_y n)} c_{p_x, p_y}. \quad (2.20)$$

The transformed Hamiltonian becomes

$$H_{LD} = \sum_{p_x, p_y} c_{p_x, p_y}^\dagger [\sin p_x \sigma^x + \sin p_y \sigma^y + (2 - m - \cos p_x - \cos p_y) \sigma^z] c_{p_x, p_y}. \quad (2.21)$$

Note that as we take the limit  $p_x, p_y \rightarrow 0$  we recover the continuum Dirac Hamiltonian from the previous section.

Now we want to couple the system to an electro-magnetic field. On a lattice we do this by adding  $U(1)$  phases on each of the lattice links *i.e.* a Peierls substitution. Again for a non-zero mass term, that is, when  $m(p) \equiv 2 - m - \cos p_x - \cos p_y \neq 0$  the system has a broken parity symmetry. Here the symmetry is broken explicitly for all values of  $m$  since  $m(p)$  never vanishes for all  $(p_x, p_y)$ . Again we can rewrite the lattice Dirac Hamiltonian in the generic form

$$H_{LD} = \sum_{p_x, p_y} c_{p_x, p_y}^\dagger d_a(p) \sigma^a c_{p_x, p_y} \quad (2.22)$$

$$d_a(p) = (\sin p_x, \sin p_y, m(p)) \quad (2.23)$$

which will be useful later. Now we integrate out the fermions, as we did for the continuum model, to get an effective action depending on the electro-magnetic field. If we calculate the parity violating terms in the polarization kernel, as we did earlier, we find a Hall conductance

$$\sigma_{xy} = \frac{1}{4\pi^2} \int_{BZ} d^2 p \epsilon^{abc} \hat{d}_a \frac{\partial \hat{d}_b}{\partial p_x} \frac{\partial \hat{d}_c}{\partial p_y} \quad (2.24)$$

$$= \frac{1}{4\pi^2} (2\pi n) = \frac{n}{2\pi} = \frac{ne^2}{2\pi\hbar} = n \frac{e^2}{h} \quad (2.25)$$

where we have used the fact that the integrand is of a special winding number form and equal to an integer multiple of  $2\pi$  when integrated over a compact manifold. The Brillouin zone (BZ) is a torus, which is compact, and thus the integral gives us  $2\pi n$ . This calculation is valid for any lattice models with Hamiltonians of the form Eq. 2.22. Generally, the integer value  $n$  is the first Chern-number of a fiber bundle defined over the BZ torus. For more complicated models the integral form Eq. 2.24 is

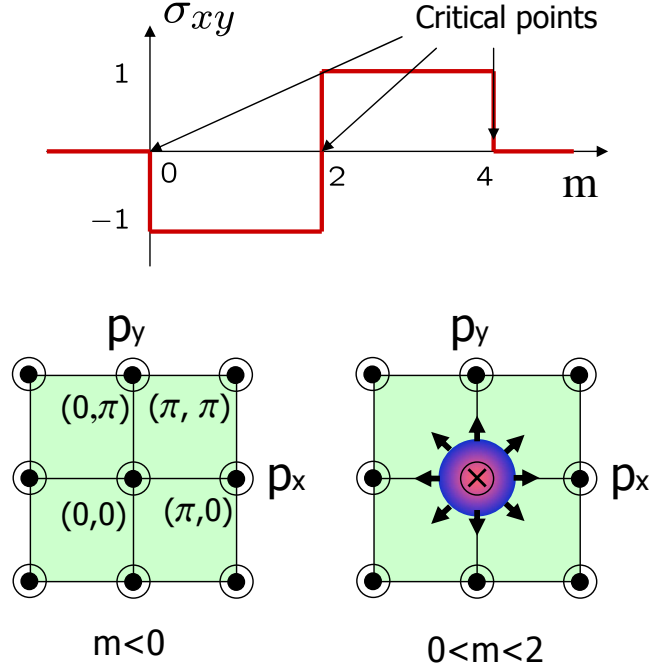


Figure 2.2: (upper) A plot of the quantized Hall conductance in units of  $e^2/h$  of the lattice Dirac model as a function of the mass parameter  $m$ . (lower) Two schematic plots of the  $\hat{d}(p)$  unit vector field for the lattice Dirac model. The left configuration has Hall conductance zero and no skyrmion charge. The right configuration has Hall conductance  $-e^2/h$  and a skyrmion charge of  $-1$ . The schematic indicates the  $z$ -component at special momentum points as well as the in-plane components if the  $z$ -component is vanishing.

no longer valid, but the integer is still the first Chern number of a more complicated bundle structure over the BZ.

Something interesting happens in the lattice Dirac model as we vary the mass parameter  $m$ . As seen in Fig. 2.2 the quantized Hall conductance depends on  $m$ . When  $\sigma_{xy}(m)$  changes values there is a topological phase transition between insulating phases. If  $\sigma_{xy}(m) = 0$  we say the system is a trivial insulator and if it is non-zero the system is in a topological insulator state. For the lattice Dirac model it is easy to understand the phase diagram by considering the low-energy physics. As a function of  $m$  the only low-energy parts of the spectrum are around the four momentum points

	$m < 0$	$0 < m < 2$	$2 < m < 4$	$m > 4$
$(0, 0)$	1/2	-1/2	-1/2	-1/2
$(\pi, 0)$	-1/2	-1/2	1/2	1/2
$(0, \pi)$	-1/2	-1/2	1/2	1/2
$(\pi, \pi)$	1/2	1/2	1/2	-1/2
$\sigma_{xy}$	0	-1	1	0

Table 2.1: Hall conductances (in units of  $e^2/h$ ) for each of the fermion flavors and the total Hall conductance for various ranges of  $m$

$(0, 0)$ ,  $(\pi, 0)$ ,  $(0, \pi)$ , and  $(\pi, \pi)$ . We can reduce our study of the entire BZ to just low-energy expansions about these four points. This effectively gives us four flavors of Dirac fermions. The low-energy Hamiltonians are

$$(0, 0): H_1(p) = p_x \sigma^x + p_y \sigma^y - m \sigma^z \quad (2.26)$$

$$(\pi, 0): H_2(p) = -p_x \sigma^x + p_y \sigma^y + (2 - m) \sigma^z \quad (2.27)$$

$$(0, \pi): H_3(p) = p_x \sigma^x - p_y \sigma^y + (2 - m) \sigma^z \quad (2.28)$$

$$(\pi, \pi): H_4(p) = -p_x \sigma^x - p_y \sigma^y + (4 - m) \sigma^z. \quad (2.29)$$

Due to the simple form of the lattice Dirac model these four flavors of fermions are the only low-energy degrees of freedom which participate in the topological phase transitions. Using our sum rule for Hall conductances of multiple fermion flavors we can construct a table of total Hall conductance (see Table 2.1). We can also look at the momentum space topological configuration for different values of  $m$ . We see two examples of these configurations in Fig. 2.2. For the trivial insulator case we see there is no skyrmion, the configuration is simply ferromagnetic-like. In the non-trivial case there is a full skyrmion in the BZ which has a charge of  $-1$  in this case giving a Hall conductance of  $-e^2/h$  for  $0 < m < 2$ .

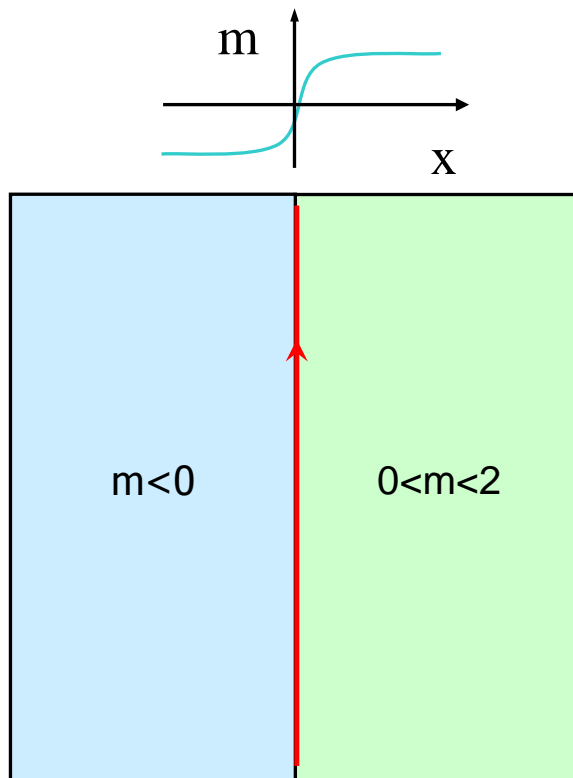


Figure 2.3: This figure shows the lateral interface geometry from which we calculate the low-energy interface states. The red line indicates the position and dispersion of the chiral interface states. The left insulator is trivial, the right one is non-trivial. The plot of  $m$  vs.  $x$  indicates a mass domain-wall at the interface.

### 2.1.2 Edge States and Domain Wall Fermions of the Dirac Model

In this section we will analyze the edge state structure of the non-trivial phase of the Dirac insulator. To begin we will study a lateral interface between two Dirac insulators, one with  $m < 0$  and one with  $0 < m < 2$ . As seen in Fig. 2.3 one of the insulators has a Hall conductance 0 and the other has  $-e^2/h$ . The integer characterizing the Hall conductance is a topological invariant and cannot change continuously. Thus as we move from left to right, interpolating between the trivial

and non-trivial insulator, we must intersect some gapless region. If we did not hit such a singularity then the two insulators could be adiabatically connected which leads to a contradiction.

The region of gapless excitations is localized around the interface and we will study the nature of the low-energy excitations. We assume that our system is translationally invariant along  $y$  so that  $p_y$  is a good quantum number. For an interface between  $m < 0$  and  $0 < m < 2$  we know from the previous section that the only significant bandstructure changes are occurring near  $(p_x, p_y) = (0, 0)$  so we will expand the Hamiltonian around this point. The other parts of the bandstructure are gapped and at higher energies. The effective Hamiltonian is

$$H(p_y) = -i \frac{\partial}{\partial x} \sigma^x + p_y \sigma^y + m(x) \sigma^z. \quad (2.30)$$

This Hamiltonian is parameterized by  $p_y$  so we will first look for an interface bound-state at  $p_y = 0$ . The bound-state ansatz we choose is

$$\psi = e^{-\int_0^x m(x') dx'} \phi_0 \quad (2.31)$$

for a constant two-component spinor  $\phi_0$ . Since  $m \sim 0$  at the interface we will look for a state with an energy  $E = 0$ . The eigenvalue equation becomes

$$H\psi = E\psi = 0 \quad (2.32)$$

$$\begin{pmatrix} m(x) & im(x) \\ im(x) & -m(x) \end{pmatrix} \phi_0 = 0 \quad (2.33)$$

$$\implies \phi_0 = \frac{1}{\sqrt{2}} \begin{pmatrix} 1 & i \end{pmatrix}^T. \quad (2.34)$$

Now we can use a trick to solve for the energies for all  $p_y$ . Since  $\sigma^y \phi_0 = +\phi_0$  we can simply let  $E = p_y$  and the Schrodinger equation is automatically satisfied! This means that there are low-energy fermion bound-states, exponentially localized on the interface, with an energy dispersion

$$E = +p_y. \quad (2.35)$$

This dispersion is simply a line with positive slope and represents a  $(1 + 1)$ -d *chiral* fermion propagating on the interface. If we exchanged the two insulators so that we had a non-trivial insulator on the left and a trivial one on the right then the dispersion would change to  $E = -p_y$  which is a chiral fermion travelling in the opposite direction.

Now instead of an interface we will put the lattice Dirac model on a cylinder of circumference  $L$ , which has two boundaries. We will orient the cylinder so that the  $y$ -direction is periodic and the  $x$ -direction is bounded. We can think of the vacuum outside the cylinder as being adiabatically connected to a *trivial* Dirac insulator with a mass  $m < 0$ , since the vacuum has  $\sigma_{xy} \equiv 0$ . Thus, the boundaries of the cylinder each contain a chiral fermion. We can physically probe these edge states by threading flux into the hole of the cylinder. If we begin to thread flux over a period of time from  $t = 0$  to  $t = T$  then we must generate a circulating electric field due to Faraday's law

$$\oint E \cdot d\ell = -\frac{\partial\Phi}{\partial t} \quad (2.36)$$

$$\begin{aligned} \implies -\int_0^T \oint \frac{dA}{dt} \cdot d\ell &= -\int_0^T dt \frac{d\Phi}{dt} \\ \implies \oint \Delta A \cdot d\ell &= \Delta\Phi = \frac{h}{e} \\ \implies \Delta A_y &= \frac{h}{eL} \end{aligned} \quad (2.37)$$

where we have threaded a single flux quantum  $\Phi_0 = h/e$  and chosen a gauge where  $\mathbf{A}(x, y, t) = (0, A_y(t))$ . We know our system has a Hall conductance of  $-e^2/h$  so there is a response during the flux threading due to the circulating  $E$  field

$$j_x = \sigma_{xy} E_y = -\sigma_{xy} \frac{dA_y}{dt} \quad (2.38)$$

$$\begin{aligned} \implies \Delta Q &= \int_0^T dt \int dy j_x = -L \int_0^T \sigma_{xy} \frac{dA_y}{dt} \\ &= L \frac{e^2}{h} \Delta A_y = \frac{e^2}{h} \frac{Lh}{eL} = e = -(-e). \end{aligned} \quad (2.39)$$

This argument clearly shows that upon inserting one flux quantum a single electron is transferred from the right edge of the cylinder to the left edge. This is a signature

2.1. DIR

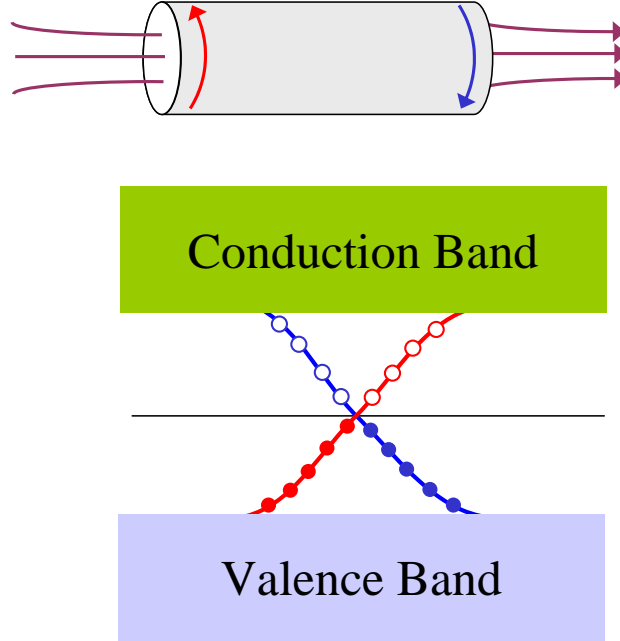


Figure 2.4: (upper) Schematic illustration of the cylinder with open boundaries along  $x$  and periodic boundary conditions along  $y$ . Red and blue lines indicate edge states on the left and right edges respectively. Purple lines indicate flux threading through the cylinder hole. (lower) Edge state dispersions and state occupations. The red line is the edge state on the left of the cylinder, the blue line is the edge state on the right of the cylinder. Empty/filled circles represent un-occupied/occupied states. During flux threading of one flux quantum the states on the red (blue) curve will shift to the right one unit causing one more state to be occupied (unoccupied).

of the IQHE.

There are two other nice ways to understand this phenomenon. First we can look at the edge state energy spectrum in Fig. 2.4. One of the dispersion lines is on one edge, while the other dispersing line is on the opposite edge. When we adiabatically thread flux the momentum of the states is shifted as

$$\begin{aligned}
 p_y &\rightarrow p_y + e\Delta A_y \\
 &= \hbar \frac{2\pi q}{L} + e \frac{h}{eL} = \hbar \frac{2\pi(q+1)}{L}.
 \end{aligned} \tag{2.40}$$

From this we see that for every flux quantum inserted the momentum each state is shifted by one unit to the right. From the energy spectrum diagram, if we shift a right moving chiral fermion then one more state is occupied, while a left moving chiral fermion has one less state occupied. Since the right mover is on the left edge, and vice-versa, we see that one electron has travelled from the right edge to the left edge. Physically the right edge is pumping an electron to the bulk, and the left edge is withdrawing one electron from the bulk.

The other way to consider this effect is by looking at the chiral fermion intrinsically as a  $(1 + 1)$ -d system. Chiral fermions in  $(1 + 1)$ -d have a classical chiral symmetry which is broken at the quantum level. Thus, it suffers from a chiral anomaly. Mathematically this means that there is a chiral (also called axial) current  $j_\mu^5$  with  $\partial^\mu j_\mu^5 = 0$  classically but

$$\partial^\mu j_\mu^5 = \frac{e}{4\pi\hbar} \epsilon^{\mu\nu} F_{\mu\nu} = \frac{e}{2\pi\hbar} (\partial_0 A_1 - \partial_1 A_0) \quad (2.41)$$

$$= -\frac{e}{2\pi\hbar} E_1. \quad (2.42)$$

Now we will apply an electric field along the length of the  $1d$  system by letting  $A_1$  vary with time. As in the previous cases we will suppose that over a period of time from  $t = 0$  to  $t = T$  we have  $\Delta A_1 = h/(eL)$ . Now we can calculate the anomalous charge

$$N_R - N_L = \int_0^T dt \int dx_1 \partial^\mu j_\mu^5 \quad (2.43)$$

$$= \int dx_1 \Delta A_1 \frac{e}{2\pi\hbar} = \frac{Lh}{eL} \frac{e}{2\pi\hbar} = 1. \quad (2.44)$$

This means, that since we only have one species of chiral fermion on a single edge, that, for example, an extra right-mover appears out of *nowhere*. The proper way to look at this is as the edge of a  $2d$  system where we know that the charge is really coming from the opposite edge.

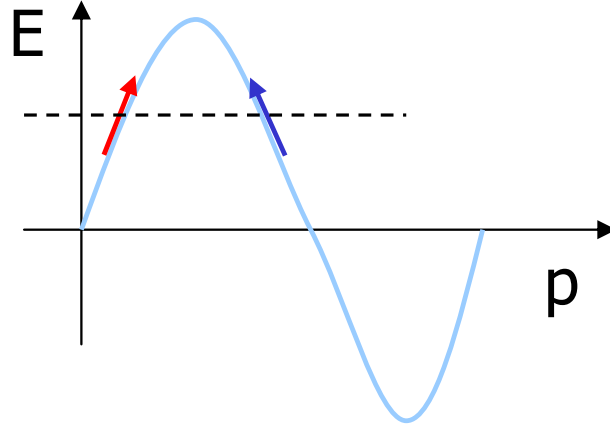


Figure 2.5: Figure illustrating a periodic dispersion relation plotted on a  $1d$  Brillouin zone. The sloped arrows represent the low-energy right and left moving chiral fermions based around the Fermi level (dotted line). No matter where you draw the Fermi level there are always an even number (possibly zero) of chiral fermions.

### 2.1.3 Holographic Liquids

We have been studying the phases of the lattice Dirac model and found that when the Hall conductance is non-vanishing the system has chiral edge states. However, there is a theorem, the Nielsen-Ninomiya theorem[17, 18], which states that we cannot get chiral fermions by themselves in a lattice model. We can imagine a simple heuristic proof aided by Fig. 2.5. The simplest example is a lattice model in  $(1+1)$ -d with a BZ which is a circle. The energy spectrum must be periodic on the circle and so if we have a right moving fermion with a positive slope, we must eventually have a left moving one with negative slope so that the spectrum is periodic. The simple statement is that, for periodic functions, what goes up must come down. The minimum amount of chiral fermions we can have is *two*: a chiral fermion and its anti-chiral partner. This has the implication that we cannot simulate chiral fermions by themselves in a lattice model.

However, topological insulators provide the one exception to this. If one wants to

simulate chiral fermions on a lattice in  $(2n)$ -d (even spacetime dimensions are required to define chirality) then simply write down a lattice Dirac model in  $(2n + 1)$ -d with a boundary and tune the mass parameter such that the system is in a topological phase. The boundaries can now contain single chiral fermions. These chiral fermions are “holographic” in the sense that they cannot exist on their own, but must appear as the boundary of some higher dimensional bulk model. Such holographic liquids are a generic property of topological insulators but the fermions do not always have to be chiral. There are other examples of holographic liquids that we will see later which cannot exist on a lattice without doubling unless they are on the boundary of a topological insulator, but which are not chiral.

## 2.2 Dimensional Reduction to $(1 + 1)$ -d

In this section we will discuss how to go from the IQHE in  $(2 + 1)$ -d to a  $(1 + 1)$ -d topological insulator. Suppose we again start with a cylinder with periodic boundary conditions along  $y$  and open boundary conditions along  $x$ . We imagine having the lattice Dirac model defined on a square lattice on the cylinder, and since we have periodic boundary conditions in  $y$  we can partially Fourier transform the fields from  $\psi(x, y) \rightarrow \psi_{p_y}(x)$ . These fields are effectively one-dimensional fields which depend on a parameter  $p_y$  as does the Hamiltonian  $H_{p_y}(x)$ . If we couple the system to an electro-magnetic field and choose a gauge such that  $\mathbf{A}$  also does not depend on  $y$ , then the Hamiltonian depends on  $H(x, p_y + eA_y(x, t), A_0(x, t), A_x(x, t))$ . Then we simply imagine replacing  $L(p_y + eA_y(x, t))$  by an inhomogeneous parameter  $\theta(x, t)$  where  $L$  is the system size in the  $y$ -direction. This will leave us with a Hamiltonian describing an inhomogeneous  $1d$  system which depends on an adiabatically varying parameter  $\theta(x, t)$ .

There is a nice heuristic picture of this formal construction in terms of compactification, or dimensional reduction. On our cylinder the fermionic fields are of the

form

$$\psi(x, y) = \sum_{p_y} e^{ip_y y} \psi_{p_y}(x) = \sum_{n=-\infty}^{\infty} e^{(2\pi i n/L)y} \psi_n(x). \quad (2.45)$$

To make the system quasi-1d we want to make sure nothing depends on the  $y$ -direction. In order to do this for the fields we must only choose the zero-mode *e.g.*  $\psi_0(x)$  which does not depend on  $y$ . Note that the energy of the fermion fields contains gradient terms which are proportional to  $1/L$ . Thus, to project onto the zero-mode we simply need to shrink the circumference of the cylinder to zero. All of the fermion modes which depend on  $y$  will be gapped and pushed to higher-energy. To handle the external electromagnetic fields we make a judicious choice of gauge so that  $\mathbf{A}$  does not depend on  $y$ . Thus in the limit  $L \rightarrow 0$  the only low-energy degrees of freedom left are  $\psi_0(x)$  and  $A_0(x, t), A_x(x, t), A_y(x, t)$ . As we did earlier we rename  $A_y(x, t) \sim \theta(x, t)/L$ . In our dimensional reduction picture  $\theta$  is effectively the amount of flux threading through the hole of the cylinder as we shrink it. We have

$$\int A \cdot d\ell = \int_0^L A_y(x, t) dy = \Phi(t) \quad (2.46)$$

which implies if  $A_y(x, t) = A_y(t)$  then  $\Phi(t) = A_y(t)L = \theta(t)$ . So in this picture to go from the QAHE/IQHE to the (1 + 1)-d topological insulator we simply construct the system on a cylindrical geometry and shrink the cylinder into a wire. The  $\theta$  adiabatic parameter is related to the “flux” threaded through the cylinder hole.

In (2 + 1)-d we had a topological term in the effective action, the Chern-Simons term

$$S_{eff}[A] \sim \int d^3x \epsilon^{\mu\sigma\nu} A_\mu \partial_\sigma A_\nu. \quad (2.47)$$

However our dimensional reduction algorithm removes any dependence on  $y$  which

means that  $\partial_y \equiv 0$  and the thin cylinder has a response

$$S_{eff}[A] \sim \int dt dx dy A_y \epsilon^{ab} \partial_a A_b \quad a, b = 0, x \quad (2.48)$$

$$= \int dx dt \theta(x, t) \epsilon^{ab} \partial_a A_b. \quad (2.49)$$

This is an example of a so-called topological  $\theta$ -term which has analogs in higher dimensions. Next, we can work out the electro-magnetic response by taking the functional derivative to get

$$j^a = \epsilon^{ab} \partial_b \theta(x, t) \quad (2.50)$$

$$j^0 = -\frac{\partial \theta}{\partial x} \quad (2.51)$$

$$j^1 = \frac{\partial \theta}{\partial t} \quad (2.52)$$

which is just the Goldstone-Wilczek formula[19]. We can also connect these formulae to  $1d$  electro-dynamics by identifying  $\theta$  with the physical charge polarization. In conventional electromagnetism we have

$$j_0 = -\nabla \cdot P = -\frac{\partial P}{\partial x} \quad (2.53)$$

$$j_1 = \frac{\partial P}{\partial t} \quad (2.54)$$

which has the same form as the Goldstone-Wilczek equations for  $\theta$ . From the construction so far we see that the  $(2+1)$ -d topological insulator is connected, via dimensional reduction, to a  $1d$  system parameterized by  $\theta(x, t)$  which can have a non-trivial electromagnetic response if  $\theta$  is not constant. This is not enough to establish the existence of a stable topological insulator phase in  $1d$  but it is at least a hint that something interesting is happening.

### 2.2.1 Topological Phase in (1 + 1)-d

One question we have not addressed is the fate of the edge states when we perform the dimensional reduction. If we generically perform the dimensional reduction for any flux threaded through the cylinder then the edge states will have no remnants in the  $1d$  insulator. In the energy spectrum, the dimensional reduction effectively projects onto a single  $p_y$  value so that only one state on the right edge and one state on the left edge remain per chiral edge state. Since these states are now disconnected from the bulk bands we can add perturbations to the ends of the  $1d$  system in a way such that the states move around in energy. By doing this we can adiabatically connect to a trivial insulator without any remaining evidence of the chiral states. This is discouraging, but there is an easy way to fix the problem. The solution is to require that our  $1d$  system satisfy an additional symmetry, in this case, a particle/hole or charge conjugation symmetry. This symmetry requires that every state at energy  $E$  must have a partner at  $-E$  unless the state is at exactly  $E = 0$ .

If we begin with a  $(2 + 1)$ -d topological insulator with one chiral branch on each edge then in the  $1d$  system each end will have a single state. Each end of the  $1d$  system is separated by some distance and we must consider them separately as long as the Hamiltonian is local. Because of the particle/hole symmetry we are enforcing, the single end states must be at exactly  $E = 0$ . Thus, since the bulk insulating gap must open symmetrically around  $E = 0$  for a particle/hole symmetric insulator, the end states are mid-gap states. Now if instead our  $(2 + 1)$ -d insulator had two branches of chiral fermions on each edge then we would get two mid-gap zero energy states on each end of the wire. However, this is qualitatively different than the previous case because we can add a perturbation that couples the pair of states on a single end. The perturbation can open a gap on each end in a particle/hole symmetric way such that we can remove any mid-gap states by pushing them high in energy. Once this has been done we can adiabatically connect the resulting state to a trivial band insulator. We cannot do this if there are mid-gap states locked at zero energy. There is clearly an even-odd effect occurring here and it turns out that the  $1d$  topological insulators with particle/hole symmetry are classified by an even/odd or  $Z_2$  topological invariant.

We have seen that if our  $1d$  insulator descends from a  $2d$  IQHE with an even or odd

number of chiral edge modes then we get different classes of  $1d$  insulators. In the end, the dimensional reduction is an artificial device and we would like an intrinsically  $1d$  way to distinguish the phases. It turns out that the value of  $\theta$  exhibited by a material gives us a way to do this. We identified  $\theta$  with the physical charge polarization earlier. On a lattice the charge polarization is only well defined up to an integer multiple of the lattice constant so  $\theta$  is only well defined up to an integer, *i.e.*  $\theta \equiv \theta + n$ . Now, under the particle/hole symmetry  $\theta \rightarrow -\theta$  since it is the charge polarization. If we want our system to be particle/hole symmetric we must have  $\theta = -\theta$  but this only has to hold up to an integer so we get two allowed values  $\theta = 0, 1/2$ . We want to identify the trivial particle/hole symmetric insulator with  $\theta = 0$ , and the non-trivial topological insulator with  $\theta = 1/2$ . We can test the consistency of these identifications by looking at a  $1d$  wire with open boundaries. The vacuum would be a trivial insulator and so at the interface between a trivial insulator wire and the vacuum there would be charge

$$Q = \int dx \nabla \theta(x) = 0 \pmod{Z}. \quad (2.55)$$

This means that the charge residing on the end of a trivial insulator is an integer multiple of the electron charge. For the topological insulator we have

$$Q = \int dx \nabla \theta(x) = 1/2 \pmod{Z}. \quad (2.56)$$

which implies that  $e/2$  charge plus an integer charge reside on the boundary. This is physically correct because the topological insulator will have an odd number of mid-gap zero modes. These zero modes contribute  $\pm e/2$  charge as seen in [20, 21]. Thus, by calculating the charge polarization of a  $1d$  particle/hole symmetric insulator we can identify the proper insulating phase.

We mentioned earlier that the Hall conductance was given by the first Chern number which is generically defined as

$$C_1 = \frac{1}{2\pi} \int d^2p \text{Tr} [\nabla \times \mathbf{a}] \quad (2.57)$$

$$(\mathbf{a})_{ij} = -i \langle u_i(p) | \partial_{\mathbf{k}} | u_j(p) \rangle \quad (2.58)$$

where  $(\mathbf{a})_{ij}$  is the non-Abelian adiabatic connection and  $u_i(p)$  are the Bloch functions of the occupied bands. The Chern number is nothing but the flux of this non-Abelian vector potential passing through the BZ. In  $1d$  the topological invariant is the zeroth Chern-Simons form

$$\theta = \frac{1}{2\pi} \int dp \text{Tr} [a_p] \quad (2.59)$$

where  $a_p$  is the only component of the adiabatic connection in  $1d$ . The Chern-Simons form is not gauge invariant if we change the phases of the Bloch functions in its definition. This is the reason why  $\theta$  is only defined modulo an integer whereas  $C_1$  is always precisely defined.

### 2.2.2 Generic Pattern for Topological Insulators

Now that we have seen a clear example of a topological insulator and a lower dimensional descendant I will outline the generic structure of the insulator families.

1. Start in  $(2n + 1)$ -d spacetime dimensions to get a real-space Chern-Simons term in the effective action by integrating out massive Dirac fermions coupled to an electro-magnetic field:

$$S_{eff}[A] = \int d^{2n+1}x \epsilon^{a_1 a_2 \dots a_{2n+1}} A_{a_1} \partial_{a_2} \dots \partial_{a_{2n}} A_{a_{2n+1}}. \quad (2.60)$$

These insulators are classified by an integer and do not require any symmetry to be stable. This integer is the  $n$ -th Chern number and is given by an integral over  $(2n)$ -d momentum space *e.g.*

$$C_1 \sim \int d^2p \epsilon^{ij} \text{Tr} [F_{ij}(p)] \quad (2.61)$$

$$C_2 \sim \int d^4p \epsilon^{ijkl} \text{Tr} [F_{ij}(p) F_{kl}(p)] \quad (2.62)$$

...

These insulators will have chiral boundary states and a topological response which can be recast into a field theory anomaly picture by focussing on the chiral fermions on a single boundary.

2. Next we perform a dimensional reduction to  $(2n)$ -d by getting rid of all of the functional dependence of  $x_{2n+1}$  and by replacing  $A_{2n+1}$  with a parameter field  $\theta(x_1, \dots, x_n, t)$ . The topological effective action will be

$$S_{eff}[\theta, A] \sim \int d^{2n}x \theta(x, t) \epsilon^{a_1 \dots a_{2n}} F_{a_1 a_2} \dots F_{a_{2n-1} a_{2n}}. \quad (2.63)$$

These states will be classified by a  $Z_2$  topological invariant instead of an integer and will require an additional symmetry restriction to maintain a stable topological phase. Our first example required a particle/hole symmetry  $C$ . Another example is the requirement of a time-reversal symmetry  $T$ . The  $Z_2$  invariant can be calculated by calculating a momentum space Chern-Simons form *e.g.*

$$\theta_1 \sim \int dp \text{Tr} [a_p] \quad (2.64)$$

$$\theta_3 \sim \int d^3p \epsilon^{ijk} \text{Tr} \left[ a_i \partial_{p_j} a_k + \frac{2}{3} a_i a_j a_k \right] \quad (2.65)$$

...

The (possibly non-linear) topological electromagnetic response here is a generalized Goldstone-Wilczek formula which requires a non-constant  $\theta$  (and possibly a non-zero electro-magnetic field too). These insulators will have gapless, but non-chiral, states on the boundary. The stability of the gapless states depends crucially on the symmetry requirement.

3. We can repeat the dimensional reduction process *exactly* one more time by adding a second inhomogeneous parameter field  $\phi$ . This second descendant is also classified by a  $Z_2$  invariant and has the same symmetry requirement as the first descendant. If we reduce again we will run into a problem which will be covered later.

### 2.3. *TOPC*

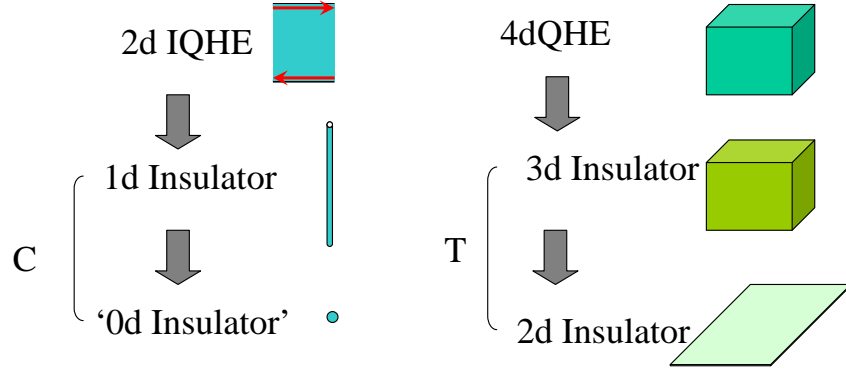


Figure 2.6: A schematic diagram showing the similarities between two different topological insulator families. The lower dimensional group requires an additional charge-conjugation symmetry  $C$  while the higher dimensional group requires time-reversal symmetry  $T$ . The two descendants in each group are classified by  $Z_2$  invariants, whereas the initial insulator in each group is classified by an integer.

## 2.3 Topological Insulator Families

After covering an explicit example of a topological insulator family we will now move on to the family in which we are most interested: the  $(3 + 1)$ -d and  $(2 + 1)$ -d TRI topological insulators. These two important systems are descendants of a  $(4 + 1)$ -d topological insulator, in the same way that the  $(1 + 1)$ -d and (although it was not discussed) the  $(0 + 1)$ -d particle/hole symmetric insulators are descendants of the IQHE. The analogy is shown in Fig. 2.6. For this family of topological insulators the required symmetry is time-reversal symmetry  $T$  with  $T^2 = -1$ . The properties of time-reversal symmetry, and Hamiltonians which preserve time-reversal symmetry, are covered in Appendix A.1. The exciting thing about this family of topological insulators, is that the strict requirement of time-reversal symmetry is not a fine-tuning problem like particle/hole symmetry would be. Time-reversal symmetry (or approximate symmetry) is a relatively robust symmetry and we could hope to find such states realized in nature *without* fine-tuning. We will see in later chapters that this is indeed the case, and I will not focus on that aspect here.

### 2.3.1 A (4 + 1)-d Topological insulator

According to the general strategy listed above I will start in  $5 = 2 \times 2 + 1$  spacetime dimensions with Dirac fermions on a hypercubic lattice. The lattice Dirac Hamiltonian with periodic boundary conditions, after being Fourier transformed, is

$$H_{LD}^4 = \sum_p c_p^\dagger \left[ \sin p_x \Gamma^x + \sin p_y \Gamma^y + \sin p_z \Gamma^z + \sin p_w \Gamma^w + \left( 4 - m - \sum_{i=1}^4 \cos p_i \right) \Gamma^0 \right] c_p \quad (2.66)$$

where  $c_p$  is a four-component spinor and the  $\Gamma^a$  are  $4 \times 4$  Dirac matrices forming a set of Clifford algebra generators. Near the point  $p_x = p_y = p_z = p_w = 0$  the lattice model reduces to the continuum model.

The next step is to couple the system to an electro-magnetic field and then integrate out the massive fermions. The topological term in which we are interested comes from the diagram in Fig. 6.7. The interesting term this diagram contributes to the effective action is

$$S_{eff}[A] = \frac{C_2}{24\pi^2} \int d^5x \epsilon^{abcde} A_a \partial_b A_c \partial_d A_e \quad (2.67)$$

where the coefficient  $C_2$  is an integer topological invariant, called the second Chern number, which characterizes the topological insulator phase. Again we can calculate the topological current response by taking a functional derivative to get

$$j^a = \frac{C_2}{32\pi^2} \epsilon^{abcde} F_{bc} F_{de}. \quad (2.68)$$

To understand what this means physically we choose a geometry with open boundary conditions along  $x$  and periodic boundary conditions along  $y, z, w$ . This is a generalization of the cylinder geometry we looked at in (2 + 1)-d. The current in the  $x$ -direction (assuming only  $F_{0y}$  and  $F_{zw}$  are non-zero) is

$$j^x = \frac{C_2}{4\pi^2} F_{0y} F_{zw} = \frac{C_2}{4\pi^2} E_y B_{zw}. \quad (2.69)$$

We can compare this to the IQHE which is  $j^x = \sigma_{xy} E_y$  which is effectively the same except for the extra factor of  $B_{zw}$  in  $(4+1)$ -d which indicates a non-linear response. This basically means that in  $(4+1)$ -d if we have a non-zero magnetic field  $B_{zw}$  we get a Hall effect.

We would also like to understand this current from an anomaly picture. The surface states of this topological insulator are chiral (Weyl) fermions restricted to the  $(y, z, w)$   $3d$  space at  $x = 0, L_x$ . When restricted to the boundary space a non-zero  $E_y \cdot B_{zw}$  is equivalent to  $E_y \cdot B_y$  since in a  $3d$  space we can associate a unique vector component  $B_y$  perpendicular to the  $zw$ -plane. The chiral current is anomalous in the presence of chiral fermions and we have

$$\partial^\mu j_\mu^5 = -\frac{e^2}{16\pi^2} \epsilon^{\mu\nu\rho\sigma} F_{\mu\nu} F_{\rho\sigma} = \frac{e^2}{2\pi^2} \mathbf{E} \cdot \mathbf{B}. \quad (2.70)$$

So when there is a non-zero  $\mathbf{E} \cdot \mathbf{B}$  applied on the surface the chiral charge is not conserved. From above we see that when restricted to the boundary, the electro-magnetic fields that give a non-zero topological response reduce to  $j^x \sim E_y B_y = \mathbf{E} \cdot \mathbf{B}$  which is exactly what we need for a non-zero anomaly. As in the lower dimensional case, the chiral anomaly on one boundary is compensated by the other boundary. These two boundaries are separated by a bulk insulator which has a non-zero topological current. A single chiral fermion in  $(3+1)$ -d on a lattice must be a holographic fermion as it was this form of chiral fermions that originally motivated Nielsen and Ninomiya.

### 2.3.2 Dimensional Reduction to $(3+1)$ -d

We can carry on with our algorithm to get the first descendant via dimensional reduction. We replace the effective action in  $(4+1)$ -d by

$$S_{eff}^{3D}[\theta, A] = \frac{1}{4\pi} \int d^3x dt \theta(x, t) \epsilon^{\mu\nu\rho\sigma} \partial_\mu A_\nu \partial_\rho A_\sigma. \quad (2.71)$$

The adiabatic parameter  $\theta(x, t)$  can still be associated to flux threaded through a hole in a higher dimensional cylinder. Also, as in the  $(1+1)$ -d case it has a physical

interpretation as a magneto-electric polarizability. It represents the amount of electric charge polarization that will result if a magnetic field is applied to the system.

We can continue with the analogy from the lower dimensional case and consider the fate of chiral edge states inherited from the  $(4 + 1)$ -d topological insulator. The Hamiltonian for the chiral edge states on the boundary of the  $4d$  system with open boundaries along the  $x$ -direction is simply

$$H = p_y \sigma^x + p_z \sigma^y + p_w \sigma^z \quad (2.72)$$

for one species of chiral fermion per boundary. This is a gapless two-band model with  $\sigma^a$  representing spin. This edge state Hamiltonian is time-reversal invariant since both momentum and spin change sign under  $T$ . The dimensional reduction process effectively picks  $p_w = 0$  and leaves us with the Hamiltonian for the surface states of a  $(3 + 1)$ -d topological insulator

$$H = p_y \sigma^x + p^z \sigma^y. \quad (2.73)$$

This is also a time-reversal invariant, gapless, two-band model for the topological surface states. In fact, this Hamiltonian is that of  $(2 + 1)$ -d Dirac fermions. Thus, when reducing we have gone from chiral fermions to Dirac fermions. If the gapless, mid-gap Dirac fermion states are stable to perturbations then we cannot adiabatically connect the resulting insulator to a trivial band insulator. However, there is a simple perturbation we can add to Eq. 2.73, that is,  $m\sigma^z$ . This term will open a small gap in the edge state spectrum. Once this small gap exists we can add surface potentials to deform the surface states into the bulk band regions in order to adiabatically connect this system with a trivial insulator.

Thus, the  $(3 + 1)$ -d topological insulator descendant is *not* generically stable. However, just like we saw in  $(1 + 1)$ -d we can fix this problem by requiring a symmetry that forbids the  $m\sigma^z$  perturbation term. This symmetry is simply time-reversal since  $\sigma^z$  changes sign, but  $m$  is unchanging. So if we require a strict time-reversal symmetry we can define a  $(3 + 1)$ -d topological insulator phase. Now suppose that our  $(4 + 1)$ -d insulator has an even number of chiral boundary fermions. This reduces down to

multiple Dirac fermion flavors in  $(3 + 1)$ -d and results in a Hamiltonian like

$$H = p_y(1 \otimes \sigma^x) + p_z(1 \otimes \sigma^y) \quad (2.74)$$

for two copies, where 1 is the  $2 \times 2$  identity matrix. Here we can add the explicit perturbation  $m(\tau^y \otimes \sigma^z)$  which will open a gap in the edge states (since it anti-commutes with the Hamiltonian) yet preserves time-reversal symmetry (since  $\tau^y$  gets complex conjugated and  $\sigma^z$  flips sign). Thus for two copies the system is no longer stable and can be connected to a trivial insulator. We once again see the signature of a  $Z_2$  classification with an even-odd type effect. We can intrinsically calculate this  $Z_2$  invariant from purely  $(3 + 1)$ -d quantities by calculating a momentum-space Chern-Simons form

$$\theta = \frac{1}{16\pi^2} \int d^3k \epsilon^{\theta ijk} \text{Tr} \left[ \left( f_{ij} - \frac{1}{3} [a_i, a_j] \right) \cdot a_k \right] \quad (2.75)$$

where  $a_i$  is the momentum-space adiabatic vector potential, and  $f_{ij}$  is its (non-Abelian) field strength. This expression is not gauge invariant, and in fact,  $\theta$  is only well defined modulo an integer. In addition, under time-reversal  $\theta \rightarrow -\theta$  so like before there are only two allowed, time-reversal invariant values  $\theta = 0, 1/2$ . A time-reversal invariant insulator with  $\theta = 0$  is trivial, and with  $\theta = 1/2$  is a non-trivial topological insulator.

We would like to show that this definition is physically consistent. The easiest way to do this is to imagine an surface between a topological insulator filling the space  $z < 0$  and the trivial vacuum filling  $z > 0$ . Thus,  $\theta = 1/2$  for  $z < 0$  and  $\theta = 0$  for  $z > 0$  leaving a  $\theta$  domain wall at  $z = 0$  (see Fig. 2.7). The topological response current is

$$j^\mu = \frac{1}{2\pi} \epsilon^{\mu\nu\rho\tau} \partial_\nu \theta \partial_\rho A_\tau \quad (2.76)$$

which is a higher-dimensional generalization of the Goldstone-Wilczek current  $j^\mu =$

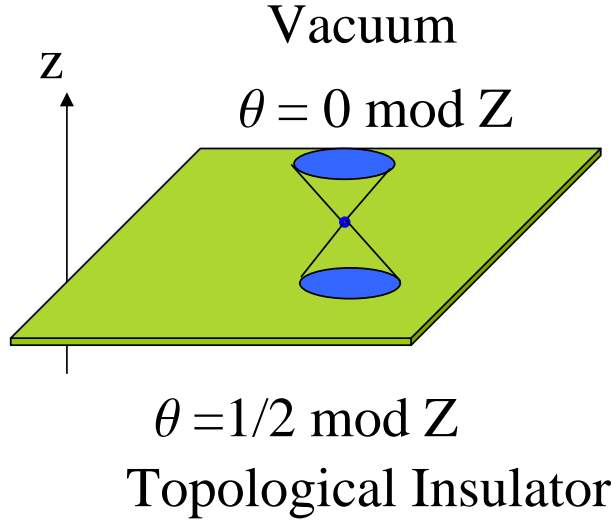


Figure 2.7: Schematic illustration of a topological insulator surface, *i.e.* an interface between the insulator and vacuum. The half Hall conductance on the surface indicates the presence of an odd number of Dirac cones localized on the surface.

$\frac{1}{2\pi}\epsilon^{\mu\nu}\partial_\nu\theta$ . Assuming  $\theta = \theta(z)$  this reduces to

$$j^\mu = \frac{\partial_z\theta}{2\pi}\epsilon^{\mu\nu\rho}\partial_\nu A_\rho \quad \mu, \nu, \rho = t, x, y \quad (2.77)$$

$$\implies j^y = \frac{\partial_z\theta}{2\pi}E_x \quad (2.78)$$

$$\begin{aligned} \implies J_{2D}^y &= \int dz j^y = \frac{E_x}{2\pi} \int \frac{d\theta}{dz} dz \\ &= \frac{E_x}{2\pi} \frac{1}{2} = \frac{e^2}{4\pi\hbar} E_x = \frac{e^2}{2h} E_x. \end{aligned} \quad (2.79)$$

Remarkably the topological response indicates that the surface of a topological insulator will carry a half-Hall conductance. This signals the presence of  $(2 + 1)$ -d Dirac fermions on the surface, which is exactly what we expect from our dimensional reduction analysis. Generically a non-vanishing  $\theta$ -term in the effective action modifies Maxwell's equations into so-called axion electrodynamics[22]. There are many striking physical consequences of this modification which are detailed in Chapter 6 and I

will defer the discussion until then.

### 2.3.3 Dimensional Reduction to (2 + 1)-d

We can perform dimensional reduction one more time to get a (2+1)-d TRI topological insulator. Before, we understood the stability of the state by examining the boundary theory. Here the edge Hamiltonian reduces to

$$H^{edge} = p_y \sigma^x \quad (2.80)$$

to which we could add two mass terms  $m_y \sigma^y + m_z \sigma^z$ . However, simply requiring time-reversal symmetry forbids both terms and we are left with a  $Z_2$  stable phase. To properly perform the dimensional reduction we have to add another adiabatic parameter  $\phi(x, t)$ . The bulk  $2d$  Hamiltonian now depends on the two parameters  $\theta, \phi$ . The topological response current of this system is non-trivial to derive (see Chapter 6), but simple to state:

$$j^\mu = \frac{1}{2\pi} \epsilon^{\mu\nu\rho} \partial_\nu \Omega_\rho \quad (2.81)$$

where  $\Omega_\rho$  is an effective Berry's phase gauge potential which depends on the inhomogeneous parameters  $\theta, \phi$ . This equation is identical to a quantum Hall response, but with real magnetic flux replaced by the Berry's phase flux. The response means that wherever we have a Berry's phase flux we have a charge. Ways to setup non-zero Berry's phase flux are given in Chapters 5 and 6. For example, if we take the edge of our system, which represents a domain-wall in  $\theta$ , and then add a magnetic domain wall on the edge, which indicates a domain-wall of  $\phi$  this will induce a charge at the intersection of the  $\theta$  and  $\phi$  domain walls. If we calculated the flux of  $\Omega_\mu$  we would find a non-zero flux located at the domain-wall intersection. This turns out to be one of the defining physical characteristics of the QSHE or (2 + 1)-d TRI topological insulator mentioned earlier.

### 2.3.4 Dimensional Reduction to $(1 + 1)$ -d

If we try to reduce the dimension again to get a TRI  $(1 + 1)$ -d topological insulator we run into a problem. It turns out that there are no stable TRI topological insulator phases in  $(1 + 1)$ -d, but at first it was unclear where the problem arises. There is a topological reason for this which is discussed in Chapter 6, but there is also a physical argument dealing with the edge states which clearly illustrates the issue.

The easiest family in which to see this problem is the insulator family starting in  $(6 + 1)$ -d. The boundary theory of this topological insulator is a chiral fermion in  $(5 + 1)$ -d with Hamiltonian

$$H = \sum_{a=1}^5 p_a \Gamma^a \quad (2.82)$$

where the  $\Gamma^a$  are  $4 \times 4$  matrices satisfying the Clifford algebra anti-commutation relation. Unlike the lower dimensional case there are other non-trivial perturbations we could add to the Hamiltonian. The space of  $4 \times 4$  Hermitian matrices has 16 basis elements: the identity 1, the 5  $\Gamma^a$  matrices, and the 10  $\Gamma^{ab} = i\Gamma^a\Gamma^b$  matrices with  $a < b$ . To destabilize a topological phase we must be able to open a gap in the edge state spectrum. The degenerate crossing point for the chiral fermion spectrum is at  $\mathbf{p} = 0$  so only the perturbations that lift the degeneracy here can cause problems. The identity matrix will not lift the degeneracy and neither will adding a constant mass term multiplying one of the  $\Gamma^a$ . It turns out that adding  $\Gamma^{ab}$  mass terms also does not lift the degeneracy, so the chiral fermion is stable. As an example we pick  $m_{12}\Gamma^{12}$ . The  $\Gamma^{12}$  term commutes with  $\Gamma^3, \Gamma^4$ , and  $\Gamma^5$ . Near the origin in momentum space the effect of  $m_{12}\Gamma^{12}$  is simply to shift the degenerate crossing point in momentum space, leaving the spectrum gapless. This is due to the commutation property mentioned above. Any  $\Gamma^{ab}$  we pick commutes with part of the Hamiltonian, and thus, only shifts the degenerate point.

Now we can consider the boundary fermion theories of the dimensionally reduced insulators. We begin with the boundary of a  $(5 + 1)$ -d descendant which will have a

Hamiltonian

$$H = \sum_{a=1}^4 p_a \Gamma^a. \quad (2.83)$$

The identity and  $\Gamma^{ab}$  have the same affect as the higher dimensional case since for each  $\Gamma^{ab}$  there is a term in the Hamiltonian with which it commutes. However, now we are free to add a term  $m_5 \Gamma^5$  which anticommutes with  $H$  and will open a mass gap. We know how to fix this problem: we require a discrete symmetry that forbids this mass term. For this family the symmetry is a pseudo-charge conjugation symmetry  $\tilde{C}$  with the property that  $\tilde{C}^2 = -1$  which is different from the conventional form  $C^2 = +1$ . This symmetry is explicitly constructed to forbid  $m \Gamma^5$ . If we go down one more dimension everything stays the same, and due to our construction,  $\tilde{C}$  also forbids the  $m_4 \Gamma^4$  term.

As discussed earlier, this should be the limit and we should run into a problem if we reduce once more. Here we would get a  $(3 + 1)$ -d insulator with a  $(2 + 1)$ -d boundary Hamiltonian

$$H = \sum_{a=1}^2 p_a \Gamma^a = p_1 \Gamma^1 + p_2 \Gamma^2. \quad (2.84)$$

We can immediately see the origin of the problem from the boundary state picture. Namely, we can now pick a special  $\Gamma^{ab}$  *i.e.*  $\Gamma^{12}$  which anti-commutes with all of  $H$ . Thus this mass term can open a gap in the boundary states. It also does so without breaking the  $\tilde{C}$  symmetry and we can connect this state to a trivial insulator state.

### 2.3.5 Summary

We have seen several examples of topological insulator families and the progression from an integer invariant to  $Z_2$  invariants. Each insulator class has its own unique topological response and holographic liquid on its boundary. The chain of stable topological insulators ends, however, after the second dimensional reduction. The different families are characterized by their spacetime dimension and the discrete symmetry

which protects the boundary states from perturbations opening a gap. The type of required symmetry repeats every 8 dimensions and hints at the deep mathematical structure underlying the classification of the topological insulator phases.